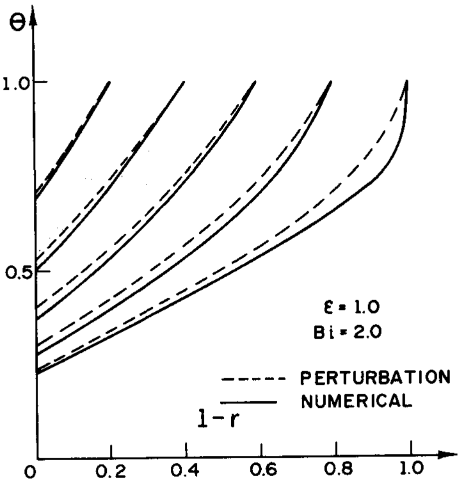

Fig. 5 Solid phase temperature profile for different interface positions.

References

[1]Tao, L.C., "Generalized Numerical Solutions of Freezing a Saturated Liquid in Cylinders and Sphere," *AIChE Journal,* Vol. 13, Jan. 1967, pp. 165–169.

[2]Milanez, L.F. and Ismail, K.A.R., "Inward Solidification of Spheres: Numerical and Experimental Analysis," ASME Paper 84-WA/HT-9, 1984.

[3]Huang, C.L. and Shih, Y.P., "A Perturbation Method for Spherical and Cylindrical Solidification," *Chemical Engineering Science,* Vol. 30, 1975, pp. 897–906.

[4]Pedroso, R.I. and Domoto, G.A., "Inward Spherical Solidification-Solution by the Method of Strained Coordinates," *International Journal of Heat Mass Transfer,* Vol. 16, 1973, pp. 1037–1043.

[5]Kucera, A. and Hill, J.M., "On Inward Solidifying Cylinders and Spheres Initially Not at Their Fusion Temperature," *International Journal of Non-Linear Mechanics,* Vol. 21, No. 1, 1986, pp. 73–82.

Roll-Out-Fin Expandable Space Radiator Concept

R. Ponnappan*
Universal Energy Systems, Dayton, Ohio
and
J. E. Beam† and E. T. Mahefkey‡
Aero Propulsion Laboratory
Wright-Patterson Air Force Base, Ohio

Nomenclature

a = area of cross section
A = external area exposed to space
b = width of the roll-out fin
C_p = specific heat capacity at constant pressure
$\dot{E}$ = rate of energy storage
F = spring force
h = fin wall thickness
h_f = specific enthalpy of fluid
h_{fg} = specific enthalpy of vaporization of the fluid
m = radiator mass
$\dot{m}$ = mass flow rate
P = pressure inside the fin
$\dot{Q}$ = heat rate
t = time
T = temperature
ΔT = temperature difference
u_g = specific internal energy
V = volume
$\dot{W}$ = rate of work done
x = length of deployment of the fin
α, β = parameters defined in Eqs. (3) and (4)
ϵ = emissivity
ρ = density
σ = Stefan-Boltzmann constant
τ = time constant

Subscripts

c = condensate
f = fin
i = input
s = sink
v = vapor

Received May 15, 1986; Presented as Paper 86-1323 at the AIAA/ASME 4th Thermophysics and Heat Transfer Conference, Boston, MA, June 2–4, 1986; revision received Sept. 23, 1986.

*Senior Scientist, Scientific Services Division. Member AIAA.

†Project Engineer, Nuclear/Thermal Technical Area. Member AIAA.

‡Technical Area Manager, Power Technology Branch. Member AIAA.

Introduction

WASTE heat rejection in space at temperatures of 300–423 K is posing technological problems for spacecraft of 100 kW capacity or more. Difficult thermal management problems lie with the high-power, low-temperature waste heat rejection associated with power processing and the payload electronic component cooling.[1] This necessitates the development of lightweight deployable radiators for future spacecraft. There are several different space radiator concepts discussed in the literature.[2–7] These concepts range from the conventional fluid loop system to the more advanced liquid droplet radiators (LDR), depending upon the temperature range and power dissipation requirements. The mass-to-power ratios $m/\dot{Q}$ of the radiators (defined as the ratio of the radiator mass to its radiating power level) are 0.017–20 kg/kW for various systems. Most of the relatively newer ideas (such as rotating spherical balloon, dust particle, glass filament, liquid droplet, direct contact belt, and single-phase external liquid flow radiators) are still in the conceptual stage. The low- or room-temperature systems have very high (orders of magnitude) mass-to-power ratios compared to the liquid metal temperature range systems.

The expandable radiator of the roll-out fin type shown in Fig. 1 contains internal vapor space and liquid condensate return channels that are primed via capillary action and the roll-up action of the spring-loaded, thin-walled, vapor chamber segments.[8] The heat transport is accomplished through the evaporation and condensation processes, while the deployment and the roll-up operations relied on the working fluid (vapor) pressure and the spring stiffness, respectively. The life expectancy of the radiator in low Earth orbits is affected by the micrometeoroid impacts. Separate research studies on survivability are required. Armor cover for the radiator in stored position, self-sealing fluid or fluid loss minimization in case of puncture, and closed-type modular fins are some of the problems to be solved. In the present study, only the feasibility of the roll-out fin concept is investigated.

Roll-Out Fin Radiator Concept

The roll-out fin radiator system can be conceived as a panel made of a number of fins mechanically working in parallel. The individual tubular segments are capable of working independently in a given pulsed (intermittant) or steady heat input condition. A group of such panels can be arranged around a vapor header as seen in Fig. 1 to form a radiator system. Two arrangements are possible to couple the fins to the primary thermal load via the vapor header. One method is the direct contact coupling where the primary fluid in the vapor header itself acts as the working fluid in the roll-out fin. This arrangement has the disadvantage of single-point failure, since a puncture in any one of the fins will result in complete fluid loss. In the other method, the primary fluid does not come in direct contact with the working fluid in the fin and the heat transfer occurs across the wall of the fin at the heat input region. This has the advantage of the meteoroid impact survivability, even though the overall thermal response of the fin may be slightly slower.

The roll-out fin, in its simplest form as shown in Fig. 2a, comprises two thin-walled sheets sealed along the edges and formed into a spiral coil. This extends due to the vapor pressure forces generated by heating the wick structure containing the working fluid. The fin curls back to the stowed position if the vapor condenses due to removal of the thermal load. The curl-back operation is used to squeeze the liquid back into the fin evaporator region where the liquid is stored in some form of a capillary wick. Maximum power dissipation occurs when the radiator fin is fully expanded and the steady-state radiated power depends on the exposed surface area, emissivity, and mean temperature. The evaporator is designed such that it does not dry out at temperatures developed by the maximum radiating power of the fin.

Design and Analysis

The scenario of space mission power requirements is diverse.[9,10] Hence, the waste heat thermal management system design approach will depend upon the specific mission. One approach is to develop a basic unit or "building block" to work in the given conditions and then arrange those units into modular configurations to build the total system. According to this approach, the basic building block of a roll-out fin or party-whistle-type radiator is the flexible fin member defined earlier. In the present subscale design, an available seam-welded, 2 mil thick, two-sheet fin, 10 cm wide and 100 cm long, has been chosen. The rate of energy radiated from the surfaces of a fully expanded fin is calculated using the laws of radiation. A design summary is shown in Table 1.

The low-temperature regime is 300–423 K and requires a radiator area to power ratio as high as 6 m^2/kW, with a minimum ratio of 1 m^2/kW. Assuming that a panel, 1×1 m is constructed out of 10 fins (of 100 W capacity each) into a module that can radiate 1 kW, we need 100 such panels to handle 100 kW of waste heat at 373 K. It can be easily seen that only 60 such panels will be necessary to radiate the same 100 kW if the temperature is 423 K.

An analysis based on a lumped thermal model is conducted to predict the dynamic behavior of the roll-out fin radiator for thermal loading. The expanded fin length as a function of time after the application of the heat load for different step input power is obtained. A control volume (CV) on the partially

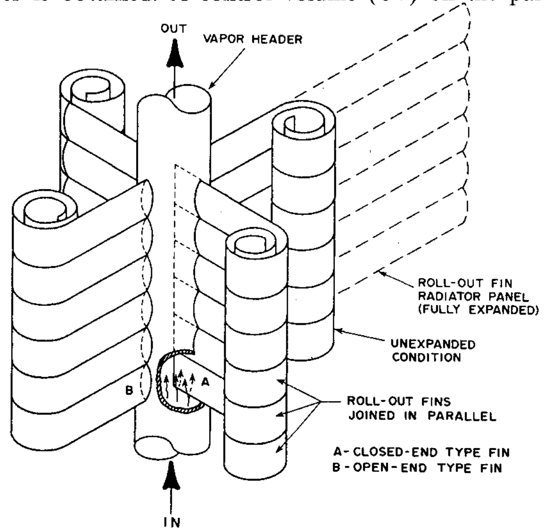

Fig. 1 Roll-out fin-type expandable radiator panel concept.

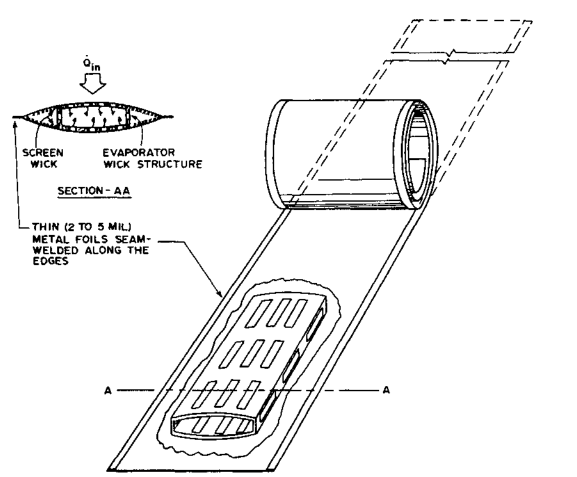

Fig. 2a Single fin unit with evaporator wick structure.

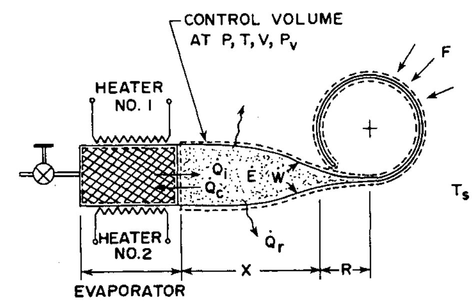

Fig. 2b Energy balance on a control volume.

expanded fin as shown in the Fig. 2b is considered. The following assumptions are made to simplify the analysis:

1) Initially at time $t = 0$, the expanded length $x = 0$ and the fluid in the evaporator wick is saturated. The fin is completely rolled and is at T_s.

2) The unrolling of the fin takes place at constant pressure and hence constant temperature. The pressure corresponds to the pressure due to the opposing coil spring force and the temperature is the saturation temperature of the fluid T_{sat} at that pressure.

3) The evaporator wick reservoir is large enough to supply vapor to the entire volume of the fin without drying up.

4) The return of the condensate is aided by the capillary mechanisms provided by the fillets along the edges of the fin in the expanded length and by the mechanical squeezing action in the coiled length. A fraction of the condensate returns to the evaporator during the expansion of the fin.

5) The heat removal from the fin is by radiation only to the sink at T_s. The thermal resistances of condensation and conduction across the thin fin walls are very small compared to that of the radiation.

6) The cross-sectional area of the expanded fin is constant.

An energy balance on the control volume gives

$$\dot{Q}_i = \dot{Q}_r + \dot{Q}_c + \dot{W} + \dot{E} \tag{1}$$

The various quantities in Eq. (1) are

$\dot{Q}_i$ = rate of energy input to the control volume $= h_{fg}\dot{m}_i$

$\dot{Q}_r$ = rate of energy radiated to sink $= 2bx\epsilon\sigma\left(T^4 - T_s^4\right)$

$\dot{Q}_c$ = rate of energy leaving due to condensate removal from the CV $= h_f \dot{m}_c$, where $\dot{m}_c$ = rate of condensate removal from the CV

$= h_f(\dot{m}_i - \dot{m}_r)$

$= h_f\left(\dfrac{\dot{Q}_i}{h_{fg}} - \rho_r a \dfrac{\mathrm{d}x}{\mathrm{d}t}\right)$, since $\dot{m}_i = \dot{m}_c + \dot{m}_r$ by mass balance

Table 1 **Roll-out fin design summary**

Material	Stainless steel 309
Construction	Two 0.051 mm (2 mil) thick foils of 10 cm × 120 cm size seam welded along the edges to form a rollable BI-STEM-like tube
Size	10 cm wide; 100 cm long (expanded) coiled to 10.16 cm diam. spiral coil with 3 turns
Radiating area	0.2 m^2 (fully expanded)
Working fluid	Water; 27 ml (18 ml in evaporator wick and 9 ml in condenser)
Temperature range	373–423 K
Power dissipation	115–167 W
Equivalent space sink	250 K
Mass-to-radiating-power ratio	0.78–0.54 kg/kW
Area-to-radiating-power ratio	1.75–1.0 m^2/kW
Mass	0.09 kg (9 ml of fluid without evaporator structure) 0.55 kg (with evaporator wick structure and 27 ml fluid)
Spring force on the spiral coil spring	3.04 N (estimated) 1.60 N (experimental) ~ 100.0 N (required)
Time constant of roll-out fin	~ 41.5 s (radiation limited)

$\dot{W}$ = rate of work done by the CV in unrolling the fin

$$= \frac{F}{a}\frac{dV}{dt} = F\frac{dx}{dt}$$

$\dot{E}$ = rate of energy storage in the CV

$$= \dot{m}_v u_g + \frac{d}{dt}\left(\dot{m}_f c_{p_f} \Delta T\right)$$

$$= \left[u_g \rho_v a + 2bhc_{p_f}\rho_f (T - T_s)\right]\frac{dx}{dt}$$

Substituting these quantities into Eq. (1) and simplifying, one obtains a first-order linear differential equation given by Eq. (2),

$$\frac{dx}{dt} + \alpha x = \beta \quad \text{with I.C.:} \quad x = 0 \text{ at } t = 0 \tag{2}$$

where

$$\alpha = \frac{2\epsilon\sigma b\left(T^4 - T_s^4\right)}{u_g \rho_v a + 2bh\rho_f c_{p_f}(T - T_s) + F - h_f \rho_v a} \tag{3}$$

$$\beta = \frac{\dot{Q}_i\left[1 - \left(h_f/h_{fg}\right)\right]}{2\epsilon\sigma b\left(T^4 - T_s^4\right)}\alpha \tag{4}$$

Equation (2) can be easily solved for x, as

$$x = (\beta/\alpha)(1 - e^{-\alpha t}) \tag{5}$$

A time constant τ which is equal to $1/\alpha$ can be defined for the exponential response of deployment of the fin radiator. The value of τ depends on the size of the fin, the fluid properties, and the operating temperature. The operating temperature in turn depends on the spring force. For a typical rollout fin, 0.1 m wide and 1 m long with a spring force of 0.1 kN (required force if water is selected as the working fluid with an operating pressure of 0.1 MPa and a temperature of 373 K), the time constant τ is 41.5 s. The expanded length x as a function of time t for several power input rates $\dot{Q}_i$ is plotted in Fig. 3 for the given fin.

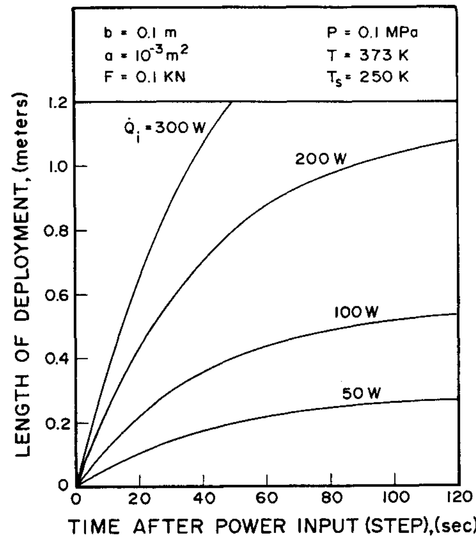

Fig. 3 Dynamic response (theoretical) of the single fin at various power inputs.

Fabrication and Testing

An available BI-STEM-like flexible fin member made of two layers of 0.051 mm thick 309 stainless steel foils seam welded along the edges was selected. The uninflated flat member was cold rolled to form a 10 cm diameter spiral coil with three turns. An 18 cm long and 9 cm wide stainless steel wick structure made of perforated stainless steel metal and four layers of 40 × 40 cm^{-1} stainless steel screen mesh was used as the evaporator wick, which was inserted from the open end of the fin after thoroughly rinsing the internal surface with alcohol. The evaporator end was fitted with a fill tube and a fill valve. The open end of the fin is closed by crimping. A unit thus sealed was connected to a heat pipe fill station and pumped down to 10^{-6} Torr and baked at 393 K for 1 h and later filled with 27 ml of water. Before filling the fin with the working fluid, it was tested pneumatically to verify the repeatability of opening and closing cycle. It was noticed that the fins expanded from the coiled position to the fully expanded position at a constant internal pressure of 760 mm Hg, while the ambient pressure was 748 mm Hg.

Thermal testing of the fin was conducted at 1 atm pressure inside a chamber, lined with cooling jacket at 277 K. Steady-state tests for power input up to 120 W (fin temperature of 370 K and deployed length of 75 cm) were carried out. The deployed length varied linearly with the steady-state power and the dynamic response fairly correlated with the prediction. The expanded length of the fin in the horizontal position supported itself and the inflated height was tapering down from the root to the tip.

Results and Discussion

An expandable roll-out fin-type space radiator segment with a mass to radiating power ratio less than 1 kg/kW has been designed. A 100 cm long and 10 cm wide stainless steel unit using water as the working fluid was fabricated to demonstrate the constant pressure roll-out and roll-in operation. This system promises application in missions of intermediate pulsed power ranges (25–100 kW) with near room temperature electronics heat rejection applications.

The initial testing conducted to date demonstrate that the device operates at steady-state condition via capillary pumping in the fillets along the seam welds. The dynamic response of the experimental unit was slower than that predicted due to its large thermal capacity. It is clear that the device offers considerable weight savings over conventional tube and fin radiators for pulsed power operation. Further study of micrometeoroid vulnerability, header/fin heat exchanger design, and operating characteristics for pulsed power input as well as vacuum and microgravity environment is required.

Acknowledgments

The work described in this paper was performed at the Air Force Wright Aeronautical Laboratories under the joint sponsorship of the U.S. Air Force Office of Scientific Research and the Aero Propulsion Laboratory. Technical help provided by Messrs. Donald Reinmuller of AFWAL and Don Brigner and John Tennant of UES is acknowledged.

References

[1]Mahefkey, E. T., "Overview of Thermal Management Issues for Advanced Military Space Nuclear Reactor Power Systems," *Space Nuclear Power Systems 1984*, Vol. 2 Orbital Book Co., Malabar, Florida, edited by M.S. El-Genk and M.D. Hoover, 1985, pp. 405–407.

[2]Leach, J.W. and Cox, R.L., "Flexible Deployable-Retractable Space Radiators," *AIAA Progress in Astronautics and Aeronautics*: *Heat Transfer and Thermal Control Systems*, Vol. 60, edited by L.S. Fletcher, AIAA, New York, 1977, pp. 243–262.

[3]Prenger, F.C. and Sullivan, J.A., "Conceptual Designs for 100 Megawatt Space Radiator," *Proceedings of a Symposium on Advanced Compact Reactor Systems*, National Research Council, Nov. 1982, National Academy Press, Washington, DC, 1983.

[4]Gedeon, L., "Description and Orbit Data of Variable Conductance Heat Pipe System for the Communication Technology Satellite," NASA TP 1465, 1979.

[5]Elliot, D.G., "Rotary Radiators for Reduced Space Power Plant Temperatures," *Space Nuclear Power Systems 1984*, Vol. 2, Orbital Book Co., Malabar, Florida, edited by M.S. El-Genk and M.D. Hoover, 1985, pp. 447–453.

[6]*Nuclear and Thermal Systems Office Monthly Report*, NASA Lewis Research Center, Nov. 1985.

[7]Chow, L.C., Mahefkey, E.T., and Yokajty, J.E., "Low Temperature Expandable Megawatt Pulse Power Radiator," AIAA Paper 85-1078, June 1985.

[8]Ponnappan, R., Beam J.E., and Mahefkey, E.T., "Conceptual Design of an 1m Long 'Roll Out Fin' Type Expandable Space Radiator," AIAA Paper 86-1323, June 1986.

[9]Taussig, R.T., "Multi-Megawatt Space Power Thermal Management System Requirements," *Space Nuclear Power Systems 1984*, Vol. 2, Orbital Book Co., Malabar, Florida, edited by M.S. El-Genk and M.D. Hoover, 1985, pp. 473–482.

[10]Mahefkey, E.T., "Military Spacecraft Thermal Management: The Evolving Requirements and Challenges," *AIAA Progress in Astronautics and Aeronautics*: *Spacecraft Thermal Control, Design, and Operations*, Vol. 86, edited by H.E. Collicott and P.E. Bauer, AIAA, New York, 1983, pp. 3–16.

Normal Spectral Emittance Data for Thoriated Tungsten, Rhenium Alloys

M. L. Ramalingam*

Universal Energy Systems, Inc., Dayton, Ohio

and

D. L. Jacobson†

Arizona State University, Tempe, Arizona

Introduction

THERE are many applications, especially in space-based power conversion systems, where high-temperature data is lacking. In an attempt to contribute to the understanding of the radiative properties of superalloys such as thoriated tungsten, rhenium alloys, the "integral method" employing an accurate photon-counting pyrometer has been used to evaluate the variation of normal spectral (0.535-μm) emittance of these alloys, with temperature as well as alloying content. The results of the experiments conducted on five thoriated (1 Mol. % ThO_2) tungsten, rhenium alloys with up to 30 at.% of rhenium revealed that the spectral emittance decreased with temperature and fluctuated with rhenium content in the temperature range of 1300 to 2300 K.

The accurate measurement of elevated temperatures was recorded by Storms and Mueller,[1] who constructed the photon-counting pyrometer capable of measuring temperatures within 1 K of the International Practical Temperature Scale. The photon-counting pyrometer was later used by Bice and Jacobson[2] to obtain emittance data at high temperatures for refractory metals such as hafnium, iridium, molybdenum, niobium, ruthenium, and tantalum. Petrov et al.,[3] determined the total emittance of molybdenum and found that it increased with an increase in temperature. The effect of change in emittance with temperature for different wavelengths of radiation was well demonstrated by Gubareff et al.,[4] who determined the existence of a certain wavelength (0.75 μm) below which emittance decreases with temperature and above which the emittance increases with temperature. This was later confirmed by Sadykov.[5]

In the photon-counting pyrometer, an interference filter allows the light energy of a particular wavelength (0.535 μm) to pass through a 0.1-mm aperture in a nickel mirror and strike the sensor in the photomultiplier tube. A photocathode sensor detects the incident radiation and converts the energy pulses to current pulses that are amplified by the discriminator-amplifier, and the timer-counter counts the current pulses per unit time, simultaneously displaying the frequency of pulses. This frequency is recorded by a thermal printer, and the recorded data is eventually converted to temperature.

The photomultiplier tube in the photon counter was tested at different threshold and excitation voltages, and the frequencies were recorded to generate a frequency-voltage plot. The plot evened out at 1.4 kV, so the tube was operated at this voltage to obtain a linear response in the expected operating temperature range. Calibration is simple, requiring the use of a single-known temperature, a variable [but an uncalibrated] source of radiation and a value for the wavelength at the transmission maximum of the interference filter. As we were interested in temperatures below 2500 K, the counter was calibrated using the melting point of copper.

The normal spectral emittance was eventually evaluated as a function of the surface and hohlraum temperatures and the pyrometer effective wavelength according to the relation

$$\epsilon_\lambda = \exp[C_c(T_s - T_h)]/\lambda T_h T_s] \tag{1}$$

where C_2 is Planck's (second) constant, λ is the pyrometer effective wavelength, and T_s, T_h are the temperatures of the surface and the hohlraum respectively, after correcting for the dead time of the counting circuits and the light attenuation factors for the various filters.

Sample Preparation and Experimental Procedure

The sample, which was heated by electron bombardment, was in the form of a disk 6.35 mm in diameter and 2.54 mm thick. Electrical discharge machining was used to drill a hohlraum with a length of 7.5 mm and a diameter of 0.75 mm in the radial direction. The repeatability of the fabrication of the hohlraum for the different samples was within 4%, maintaining a length-to-diameter ratio of greater than 9:1 in all cases. The region around the hohlraum was polished with 240-grit Carborundum wet/dry paper to provide a flat surface, the emittance of which was to be evaluated. The sample was spot-welded to a tantalum holder and mounted inside the bell jar for experimentation.

Each of the five samples was tested in a water-cooled, diffusion-pumped vacuum system with a vacuum of at least 6×10^{-6} Torr. The sample was heated till the required temperature was attained and maintained at that temperature for one hour, during which frequency measurements were

Received Sept. 24, 1986; revision received Jan. 13, 1987.

*Research Scientist. Member AIAA.

†Professor. Member AIAA.